14th International Symposium on Turbulence and Shear Flow Phenomena (TSFP14)
Heidelberg, Germany, July 28–31, 2026

INFLUENCE OF SURFACE ROUGHNESS TOPOGRAPHY ON HEAT TRANSFER IN TURBULENT FLOWS

Himani Garg
Department of Energy Sciences
Lund University
Ole Römers väg 1, 22100, Lund, Sweden
himani.garg@energy.lth.se

Karl Johan Nogenmyr
Siemens Energy AB,
Slottsvägen 2-6, SE-61283
Finspang Sweden

Alexander Stroh
Institute of Fluid Mechanics
Karlsruhe Institute of Technology
Kaiserstr. 10, 76131 Karlsruhe, Germany
alexander.stroh@kit.edu

ABSTRACT

This study models Additive Manufacturing (AM) roughness using a statistical distribution of spheres and performs high-fidelity simulations at a bulk Reynolds number of 12,000 and a large range of Prandtl numbers to evaluate heat transfer on a rough pipe. Statistical measures were deployed to highlight a clear correlation between roughness features and heat transfer. To directly connect surface topography with local heat transfer, the roughness height map was classified into quantile-based roughness zones: canyons, lower slopes, upper slopes, and tips. Probability density functions of the normalized Nusselt number in these zones reveal a clear stratification of convective performance: canyon regions exhibit the lowest heat transfer due to shielding and limited turbulent renewal, while tip regions consistently achieve the highest values through direct exposure to turbulent eddies and boundary-layer disruption. A complementary sheltering analysis based solely on surface visibility to the incoming flow distinguishes weakly ventilated regions with suppressed heat transfer from exposed windward faces that host intense thermal events. Probability density functions of the local Nusselt number based on sheltering analysis reveal pronounced spatial variability linked to surface geometry. These findings highlight the central role of roughness elevation and spatial exposure in governing turbulent heat transfer and provide new insights into the thermal–hydrodynamic behavior of AM-fabricated channels.

ROUGH WALLS HEAT TRANSFER

Additive Manufacturing (AM) allows the creation of complex geometries with high accuracy, offering significant advantages for industries like aerospace and automotive. However, the inherent surface roughness of AM processes, influenced by printing techniques and material selection, significantly affects pressure loss and heat transfer properties. The effect of surface roughness has also been investigated numerically with various methods (Kadivar & Garg, 2024). Several studies have proposed roughness models to account for roughness in laminar flows. Advancements in computer technology have facilitated Direct Numerical Simulations (DNS) for studying turbulent heat transfer over resolved rough surfaces (MacDonald *et al.*, 2019; Kuwata, 2021), indicating the dissimilarities between heat and momentum transfers were evident in the recirculation zone behind roughness elements, where effective Prandtl numbers increased rapidly within the rough surface. Recent DNS studies have investigated the scaling behavior of the temperature roughness function, $\Delta\Theta^+$, analogous to wall roughness function, ΔU^+, and observed notable deviations from the established ΔU^+ correlation, particularly at higher k_s^+ values (MacDonald *et al.*, 2019; Kuwata, 2021). To date, convective heat transfer in AM-made mini-channels remains understudied, with limited experimental and numerical investigations (Snyder & Thole, 2020; Garg & Wang, 2024; Garg *et al.*, 2024). Snyder & Thole (2020) demonstrated successful tailoring of surface roughness through AM process parameters, enhancing the performance of a generic micro-channel cooling design. More recent studies by Garg & Wang (2024); Garg *et al.* (2024) have largely focused on systematically exploring the relationship between AM roughness characteristics and k_s to reveal their impact on turbulent heat transfer using the similarity function, all-normal Reynolds stress, heat flux, and probability density functions by using wall resolved Large Eddy Simulations (LES). In this paper, we continue these studies and aim to show a direct comparison between the roughness characteristics and heat transfer by utilizing statistical methods.

METHODS

This study involves conducting wall-resolved LES of thermal flow in roughened pipes. The flow is assumed to be incompressible, Newtonian, and heated with a uniform wall heat flux q_w. The incompressible filtered Navier-Stokes equations are solved numerically using the modified solver developed in OpenFOAM based on the finite-volume method (Garg & Wang, 2024; Garg *et al.*, 2024). The roughness is constructed with a rather random distribution of many spherical structures and also some large-scale ridges and valleys, by manually identifying the spheres based on the 2 scanning electron microscope pictures. The subgrid viscosity is modeled using the Wall-Adapting Local Eddy-viscosity (WALE) model. The LES equations were solved numerically using a second-order spatial and temporal discretization schemes (Garg & Wang, 2024; Garg *et al.*, 2024). Here Pr was varied between 0.5 to 3, and the bulk Reynolds number ($Re_b = 12000$) was maintained throughout. The characteristic diameter ($D = S/\pi L_x$) is defined based on the rough surface area (S) and pipe length (L_x) Garg & Wang (2024). The computational domain length ($L_x = 4D$) ensures accurate statistics, with periodic boundary conditions in the streamwise direction and no-slip conditions at the wall. A forcing term maintains the mean pressure gradient imposing a prescribed Re_b. Friction velocity (u_τ) was calculated from the resultant pressure gradient. The statistics are gathered over 50 flow-through times after a fully-developed flow state has been reached. This setup enables a detailed analysis of turbulent flow and heat transfer over rough surfaces at fixed Prandtl and Reynolds numbers.

RESULTS

The results presented in Fig. 1 show the impact of surface roughness on wall local heat transfer Nu, normalized with the reference value from the smooth-surface pipe Nu_0. In Fig.1a, the local Nu/Nu_0 demonstrates a similar spatial variability, with high heat transfer occurring in the regions of exposed roughness elements, arises from the intensified turbulent mixing in the near-wall region, and most likely due to thermal boundary layer disruption.

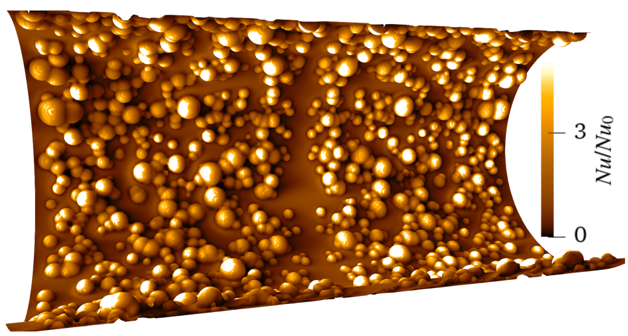

(a)

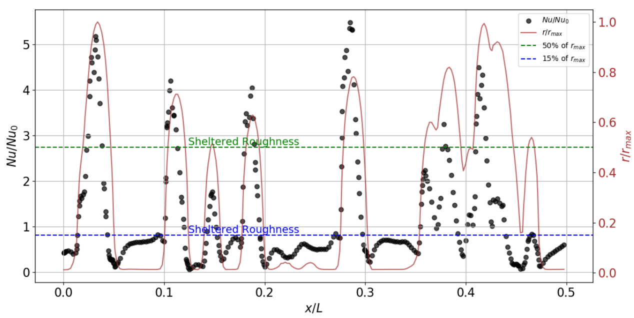

(b)

Figure 1: (a) Local Nusselt number, Nu/Nu_0, normalized by the Nu of smooth pipe flow, and (b) correlation of surface roughness height and local Nu along a line (bottom).

In Fig. 1b we show the correlation of surface roughness height and local Nu/Nu_0 along the streamwise direction. The solid line represents surface roughness height, while the point data depicts the time-averaged local Nu/Nu_0. Horizontal dashed lines indicate 50% (green) and 15% (blue) of the maximum roughness height. High Nu/Nu_0 are observed at the peaks of the roughness elements, where the elevated surface forces the flow to accelerate, promoting stronger turbulence and thermal mixing. These peaks act as zones of enhanced heat transfer, aligning with the expected impact of roughness-induced flow disruption. Conversely, a gradual decline in Nu/Nu_0 is evident when downstream roughness elements are shorter than their upstream neighbors. These "sheltered roughness" elements experience reduced exposure to the incoming turbulent flow as they are engulfed within the wake of the taller upstream roughness and avoid direct flow impingement. The flow in these regions may not reattach effectively, leading to reduced wall shear stress and diminished heat transfer. Notably, when the roughness height decreases substantially falling below 50% of the upstream roughness height, a pronounced reduction in heat transfer enhancement occurs, with values dropping below those observed in a smooth pipe. This phenomenon can be linked to the formation of recirculation zones. The taller upstream roughness elements create large separation bubbles and wakes, extending downstream.

ZONAL ANALYSIS

These observations motivate a new roughness segmentation approach for a better understanding of the roughness-induced thermohydraulic property modification. For this, the inner pipe wall was divided into quantile-based roughness zones as shown in Fig. (2).

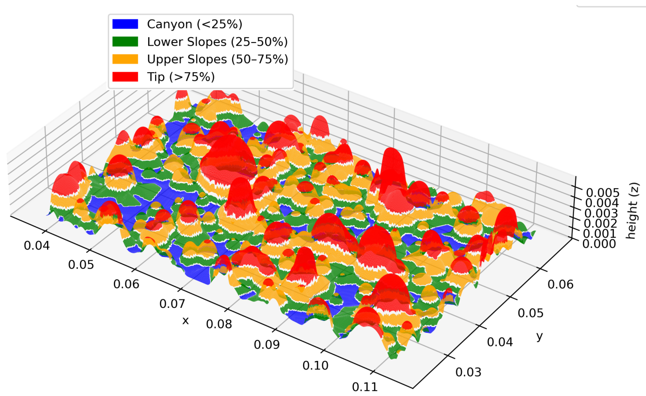

(a)

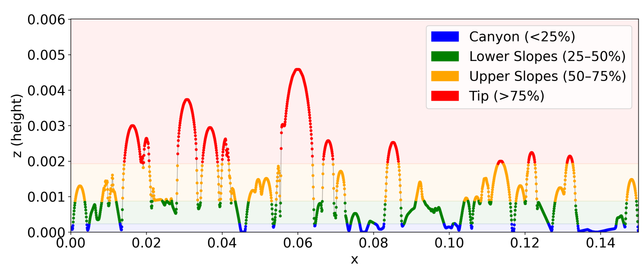

(b)

Figure 2: (a) 3D and (b) 2D view of roughness height quantile zones: canyon (blue, upto 25% of h_{max}), lower slopes (green, next 19%), upper slopes (orange, next 25%), and tip regions (red, rest of h_{max}).

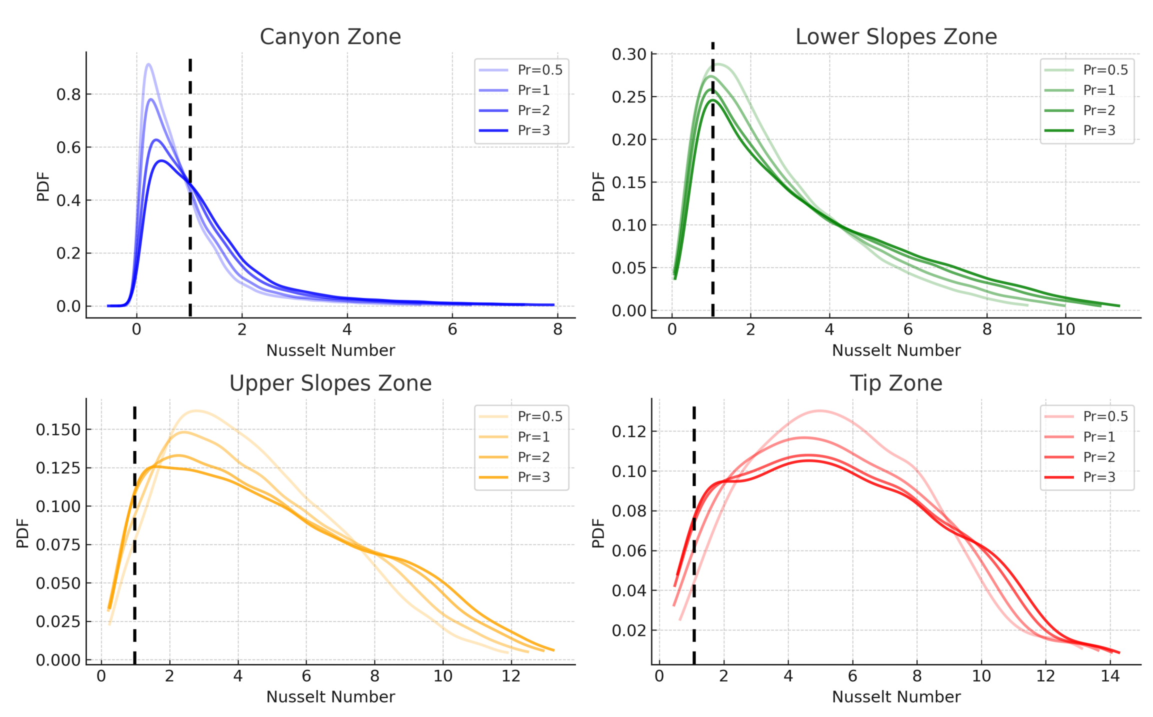

Figure 3: PDF of Nu normalized by the smooth surface value Nu_0 for different zones and different Prandtl numbers. Dashed black line is for $Nu/Nu_0 = 1$.

The classification into canyon regions, lower slopes, upper slopes, and tip regions highlights that a majority of the surface area lies in the deep canyon zones (65.5%), while the protruding tips cover 31.25% of the highest roughness range.

The probability density functions (PDFs) of the local normalized Nu/Nu_0 for different zones (Fig. 3) provide deeper insights into the role of roughness topology on convective heat transfer. For example, at a fixed Pr number (see Fig. 3,a) the canyon zones (blue) correspond to the valleys of the surface and exhibit the lowest heat transfer performance. The PDFs show a narrow distribution at low Nu/Nu_0 values, suggesting that these zones behave almost like thermally insulated areas ($Nu/Nu_0 < 1$) due to limited interaction with turbulent eddies and restricted renewal of fluid near the wall. The lower slopes (green) with their intermediate elevation perform moderately better than canyons often providing $Nu/Nu_0 > 1$. The Nu/Nu_0 distributions shift toward slightly higher values, reflecting enhanced exposure to flow structures compared to deep valleys. Still, the shielding effect from upper roughness features limits their thermal contribution. The upper slopes (orange) zones show a significantly improved convective performance. Their partial exposure to the main flow, especially on windward-facing sides, increases interaction with turbulent structures. Consequently, the Nu/Nu_0 distributions spread toward higher values, marking a transition between sheltered and fully exposed regions. While for the tip regions (red) highest convective intensities are observed at the tips. The PDFs peak at large $Nu/Nu_0 = 4-6$ with a wider spread, indicating strong spatial variability but consistently elevated heat transfer. This is linked to the protruding peaks directly intercepting turbulent eddies and acting as primary sites for energy and momentum exchange, resulting in enhanced local heat fluxes.

As the Pr number increases, the overall convective performance improves due to reduced thermal diffusivity and thinner thermal boundary layers. This enhancement is most pronounced at the tips and upper slopes, where direct exposure to turbulent eddies leads to higher and broader Nu distributions. Lower slopes show moderate gains, while the canyons remain weakly affected and concentrated at low Nu values. Thus, increasing Pr accentuates the contrast between sheltered and exposed roughness zones.

Overall, these results demonstrate a clear stratification of heat transfer efficiency with roughness elevation and highlights the importance of roughness geometry and surface exposure in controlling local transport processes in turbulent flows.

WIND SHADE SHELTERING ANALYSIS

To better connect the heat transfer behavior to the underlying roughness topography, the sheltering mechanism is investigated, i.e., the extent to which the upstream roughness features block or expose downstream surface regions to the mean flow. The procedure adopts the geometric idea used in the ”wind-shade model” of Meneveau et al. Meneveau *et al.* (2024): for each surface point, we compute whether it lies in the ”shadow” of an upstream peak based on its horizon angle. As illustrated in Fig. 4(a), for a given surface point (x,y), the backward horizon angle $\beta(x,y)$ is defined as the maximum elevation angle between the point and any upstream surface point along the mean flow direction. The turbulence spreading angle θ represents the effective angular spread over which turbulent motions can penetrate into downstream cavities. A surface point is classified as sheltered when $\beta(x,y) > \theta$, and exposed otherwise. Points with a local backward-looking angle larger than a prescribed turbulence-spreading angle are classified as sheltered, while the remainder are exposed. Full details of the drag model can be found in Meneveau *et al.* (2024). Here the geometric operator is only utilized to identify the local regions of the roughness exposed to the flow or sheltered by the upstream elements.

Figure 4 summarizes the resulting sheltered regions (pink shading) for velocity and temperature fields at different Prandtl

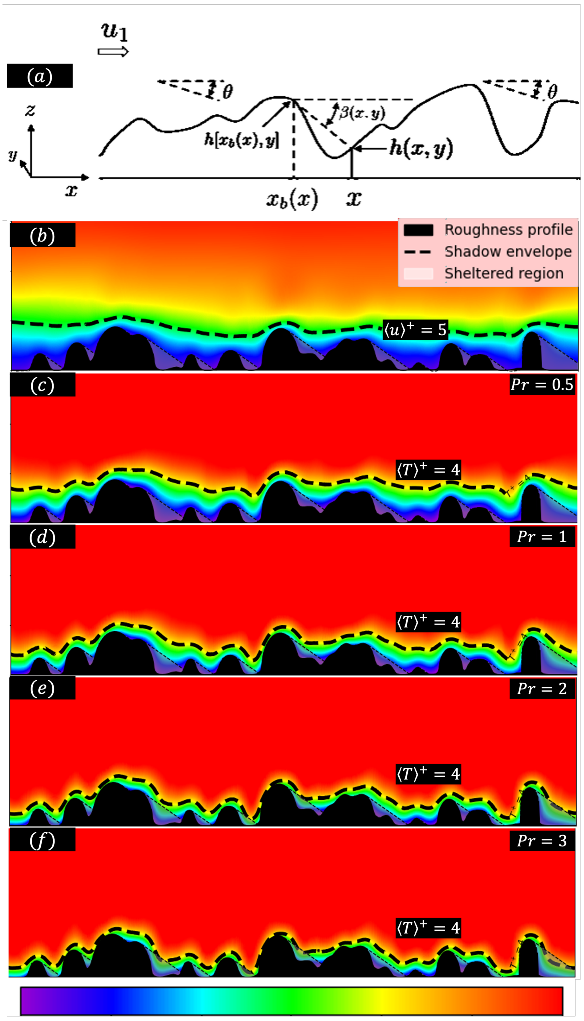

Figure 4: Sheltering due to surface roughness. (a) sketch of surface, turbulence spreading angle θ, and backward horizon angle $\beta(x,y)$ for any given point (x, y). Since in the example shown the point x has β that is larger than the turbulence spreading angle θ, point x is considered sheltered (wind-shaded). Time-averaged (b) velocity, $\langle u_x \rangle^+$, and (c-f) temperature, $\langle T \rangle^+$, for Pr = 0.5, 1, 2, and 3. Dashed thick black line corresponds to viscous and thermal boundary layer thickness.

numbers. Two main observations emerge. Firstly, across all Pr numbers, the region immediately beneath large upstream crests is characterized by suppressed temperature levels, visible as the dark-blue/green pockets aligned with the sheltered mask. These corresponds to zones where turbulent exchange with the outer flow is strongly inhibited. Because the mean flow cannot "see" into these cavities, heat transfer there is limited to weaker diffusion-dominated processes. This leads to reduced local $\langle T \rangle^+$, damping of temperature gradients, and a delayed transition from conduction-dominated to convection-dominated heat transport. This effect is structurally similar to the low-momentum pockets seen in the velocity field (panel b, Fig. 4), but it has intensified thermal contrast due to steep wall-normal temperature gradients.

In all Pr numbers considered (panels c-f, Fig. 4), high temperature gradients and enhanced $\langle T \rangle^+$ occur predominantly at points exposed by the sheltering operator. These are the intermediate upstream faces of roughness elements, which remain in direct contact with energetic turbulent motions. Heat transfer is therefore maximized on these windward slopes. This behavior parallels the role of unsheltered regions in the wind-shade drag model, i.e., exposed areas carry most of the pressure drag, here, they also carry most of the thermal flux. The analogy is strengthened by our earlier results showing that wall-normal heat-flux tracks the Reynolds shear stress almost exactly Garg *et al.* (2024). Both quantities peak where the sheltering map identifies maximum exposure.

Moreover, as Pr number increases, thermal diffusivity decreases, making temperature fluctuations more tightly coupled to the turbulent structures. This results in sharper thermal contrasts, thinner thermal sublayers, and more intense hot spots on exposed faces and sharper cold pockets within sheltered zones. However, the spatial pattern of sheltered versus exposed regions does not depend of Pr number, the geometry fixes it. What changes is the strength of the thermal imprint inside each region, for low Pr (e.g. 0.5), diffusion softens the temperature field and damps sheltering signatures, whereas for high Pr numbers (e.g. 3), the thermal gradients at the interface between sheltered and exposed regions become steeper, leading to more spatially distinct temperature patterns within the sheltered pockets. These results show that roughness-induced heat-transfer augmentation is governed not simply by element height, but by the fraction of the wall that is exposed versus sheltered.

To quantify how sheltering modifies the local heat-transfer statistics, we compute probability density functions (PDFs) of the local Nusselt (Nu) number, normalized by its smooth-wall average from correlations, Nu/Nu_0, shown in Fig. 5. The PDFs are conditioned on whether each wall point is classified as sheltered or unsheltered by the geometric criterion described above, and are also shown for all points combined (Fig. 5). For all Pr numbers, the conditional PDFs reveal a clear separation between the two regions. The unsheltered areas exhibit a broad distribution with an extended tail at large values of Nu/Nu_0, indicating frequent intense local heat-transfer events associated with direct exposure to the outer flow and strong turbulent impingement. In contrast, the sheltered regions show a much narrower distribution, strongly weighted towards low and near-unity values of Nu/Nu_0, and with substantially reduced probability of very high-Nu events. The combined PDF lies between these two conditional curves, confirming that the global enhancement of heat transfer over the rough wall is primarily driven by the relatively small fraction of unsheltered surface that supports very large local Nu numbers. Because the normalization uses the smooth-wall correlation, $Nu/Nu_0 > 1$ reflects the degree to which roughness locally enhances heat transfer relative to an equivalent hydraulically smooth configuration.

The influence of Pr number on the Nu/Nu_0 PDFs is comparatively modest. Across all Pr, the dominant separation is geometric: unsheltered regions exhibit a broad distribution with substantial probability at moderate Nu/Nu_0, while sheltered regions show a sharp peak at very low Nu/Nu_0 values, reflecting their weak exposure to turbulent transport. Increasing Pr number slightly decreases the probability density near the low-Nu/Nu_0 peak and mildly increases the probability density in the high-Nu tail for all the three curves, consistent with thinner thermal sublayers at higher Pr. However, the relative difference between sheltered and unsheltered areas remains essentially unchanged. This confirms that the primary control on local heat-transfer variability is the sheltering imposed by the roughness topography, while Pr number plays a secondary role by adjusting the diffusivity of the scalar field.

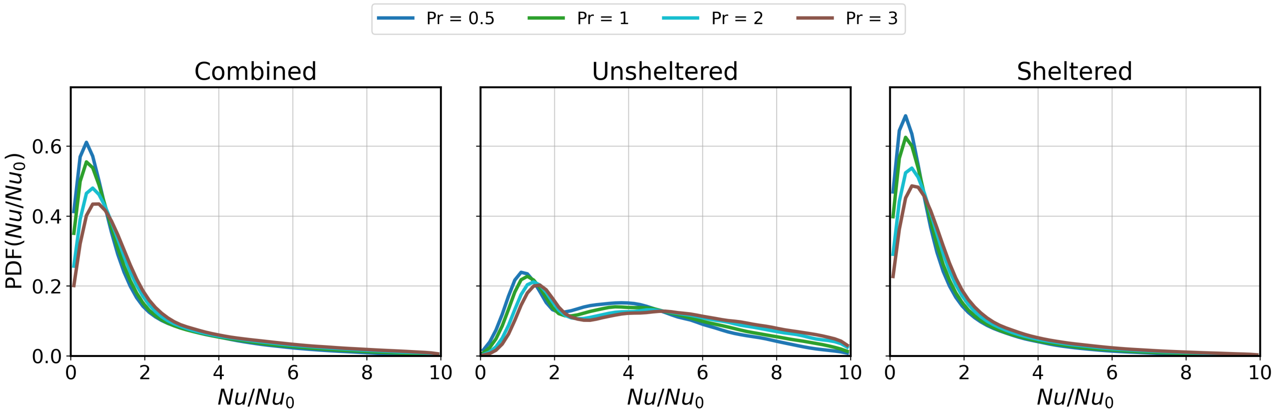

Figure 5: PDF of normalized Nu number based on sheltered and unsheltered regions for a range of Pr number.

CONCLUSIONS

The present study examined turbulent heat transfer in a rough AM pipe across a range of Prandtl numbers using a systematic combination of sheltering diagnostics and roughness-height zonal conditioning. Despite the geometric complexity of the surface, several robust and unifying trends emerged.

To reveal the geometric origins of this behavior, we introduced a zonal analysis based on roughness height, illustrated how localized topographic features modulate heat-transfer variability. While differences across height bands were moderate at low Pr, they became increasingly pronounced as Pr increased, with crest regions contributing disproportionately to high-Nusselt events. The progressive broadening of the PDFs with Pr captured the increasing sensitivity of scalar transport to the detailed structure of the turbulent motions interacting with the rough wall.

A complementary sheltering analysis inspired by the wind-shade framework has been carried out. Sheltered regions, defined purely by surface geometry, consistently exhibited weakened turbulent activity and lower temperatures, whereas exposed windward faces supported strong wall-normal heat transport. PDFs of local Nusselt numbers confirmed this partitioning: unsheltered regions displayed broader distributions and more frequent high-Nusselt events, while sheltered pockets remained dominated by weakened heat transfer. Notably, the distinction between sheltered and unsheltered areas persisted across all Pr, indicating that the geometry-imposed visibility to the flow is a primary determinant of local heat-transfer intensity.

Taken together, these results highlight a central finding of this investigation: for the present AM non-Gaussian roughness, the influence of the Prandtl number on local heat-transfer behavior, while measurable, is relatively modest compared to geometric factors such as sheltering and feauture-dependent exposure. We hypothesize that surfaces with more sharply defined or multimodal topographic features (e.g. bimodal height distributions, clustered peaks, or steep localized protrusions) are expected to exhibit a much stronger coupling between Prandtl number and local heat-transfer enhancement, due to more extreme sheltering contrasts and a more heterogeneous distribution of exposed faces. This suggests an important direction for future research. The sheltering and zonal frameworks developed here provide powerful, geometry-based diagnostic tools that could form the foundation for new heat-transfer correlations for rough surfaces. However, to generalize these tools, additional simulations spanning a broader variety of roughness statistics, including bimodal, skewed, and anisotropic surfaces, will be required. Such investigations are planned as part of our continuing effort to establish predictive, physically interpretable models for rough-wall heat transfer across a wide range of Prandtl numbers and roughness topographies.

ACKNOWLEDGMENTS

This work acknowledges the competence center AdTherM funded by the Vinnova (project no. 2023-00552) and Crafoord funding (project no. 20250841). The computations were enabled by resources provided by the National Academic Infrastructure for Supercomputing in Sweden (NAISS), partially funded by the Swedish Research Council through grant agreement no. 2026-0310, LUNARC through grant agreement no. 2026-0204. The authors also acknowledge Ambrosio Pedreno Marin for the geometry file.

REFERENCES

Garg, H., Sahut, G., Tuneskog, E., Nogenmyr, K. J. & Fureby, C. 2024 Large eddy simulations of flow over additively manufactured surfaces: Impact of roughness and skewness on turbulent heat transfer. *Phys. Fluids* **36** (8), 085143.

Garg, H. & Wang, L.and Fureby, C. 2024 Heat transfer enhancement with additively manufactured rough surfaces: Insights from large-eddy simulations. *Phys. Fluids* **36** (2).

Kadivar, M. & Garg, H. 2024 Turbulent heat transfer over roughness: a comprehensive review of theories and turbulent flow structure. *Int. J. Thermofluids* p. 100967.

Kuwata, Y. 2021 Direct numerical simulation of turbulent heat transfer on the reynolds analogy over irregular rough surfaces. *Int. J. Heat Fluid Flow* **92**, 108859.

MacDonald, M., Hutchins, N., Lohse, D. & Chung, D. 2019 Heat transfer in rough-wall turbulent thermal convection in the ultimate regime. *Phys. Rev. Fluids* **4** (7), 071501.

Meneveau, C., Hutchins, N. & Chung, D. 2024 The wind-shade roughness model for turbulent wall-bounded flows. *J. Fluid Mech.* **1001**, A3.

Snyder, J. C. & Thole, K. A. 2020 Tailoring surface roughness using additive manufacturing to improve internal cooling. *J. Turbomach.* **142** (7).